Design of Salt-Insensitive Glycine-Rich Antimicrobial Peptides with Cyclic Tricystine Structures†

James P. Tam,* Yi-An Lu, and Jin-Long Yang

Department of Microbiology and Immunology, A5119 MCN, Vanderbilt University, Nashville, Tennessee 37232-2363

Received February 15, 2000; Revised Manuscript Received April 17, 2000

ABSTRACT: Cyclic peptide backbone and cystine constraints were used to develop a broadly active salt-insensitive antimicrobial peptide [Gly_6]ccTP **1a** with eight Gly residues in an 18-residue sequence. The importance of rigidity and amphipathicity imparted by the cyclic and cystine constraints was examined in two peptide series based on tachyplesin, a known β-stranded antimicrobial peptide. The first series, which retained the charge and hydrophobic amino acids of tachyplesin, but contained zero to four covalent constraints, included a cyclic tricystine tachyplesin (ccTP **1**). Corresponding [Gly_6] analogues were prepared in a parallel series with all six bulky hydrophobic amino acids in their sequences replaced with Gly. Circular dichroism measurements showed that ccTP **1** and [Gly_6]ccTP **1a** exhibited well-ordered β-sheet structures, while the less constrained [Gly_6] analogues were disordered. Except for linear peptides assayed under high-salt conditions, peptides with increased or decreased conformational constraints retained broad activity spectra with small variations in potency of 2−10-fold compared to that of tachyplesin. In contrast, Gly replacement analogues resulted in large variations in activity spectra and significant decreases in potency that roughly correlated with the decreases in conformational constraints. Except against *Escherichia coli*, the Gly-rich analogues with two or fewer covalent constraints were largely inactive under high-salt conditions. Remarkably, the most constrained [Gly_6]ccTP **1a** retained a broad activity spectrum against all 10 test microbes in both low- and high-salt assays. Collectively, our results show that [Gly_6]ccTP **1a** could serve as a template for further analogue study to improve potency and specificity through single or multiple replacements of hydrophobic or unnatural amino acids.

Antimicrobial peptides are important components of the host defense against microbial infections (*1*−*6*). These peptides are usually cationic and possess broad-spectrum activities against bacteria and fungi through killing mechanisms such as altered permeability and pore formation that are directed against microbial membranes. Furthermore, they are known to display or have the propensity to fold as amphipathic structures with clusters of hydrophobic and charge regions. This structural property appears to be closely related to their membranolytic activity, including their activity spectrum and hemolytic selectivity. However, their activity is often abrogated under physiological conditions containing 100−150 mM NaCl (hereafter termed high-salt conditions) that limit their therapeutic applications (*5*, *6*).

Modulation of amphipathicity and hydrophobicity has been used for designing analogues and for correlating mechanisms of action (*7*−*19*). However, it is often difficult to dissociate unambiguously the sequence changes from concomitant conformational changes that affect membranolytic activity, particularly under high-salt conditions. Recently, two types of highly rigid cyclic antimicrobial peptides have been identified from natural sources (*20*, *21*). We envision that these highly constrained peptides could serve as models to minimize conformational changes and salt sensitivity in analogue activity studies.

Both types of rigid antimicrobial peptides contain a tricystine-stabilized β-stranded and end-to-end cyclic peptide backbone framework. The first type is found in plant-derived peptides that include kalata, circulin A and B, and cyclopsychotride (*22*−*25*). These cyclic peptides of about 30 amino acid residues exhibit a well-ordered framework of three β-strands stabilized by three cystine pairs in a cystine-knot motif that is commonly observed in protease inhibitors and toxins (*26*). More recently, a second type of cyclic tricystine peptide termed RTD-1 (rhesus theta defensin, Figure 1) has been identified from monkey leukocytes (*20*). RTD-1 is an 18-amino acid cyclic peptide also with a "cystine-knot"-like motif but on a two-β-strand framework. Unlike other members of the defensin family, RTD-1 is salt-insensitive.

Our need for rigid peptides to correlate conformational effects and salt sensitivity in antimicrobial peptides has led to the development of cyclic tricystine templates based on protegrins (*27*) and tachyplesins (*28*, *29*) that are structurally similar to RTD-1 (Figure 1). The synthetic template ccTP **1** (cc, cyclic cystine) based on the tachyplesin-1 (TP) isolated from the Japanese horseshoe crab (*Tachypleus tridentatus*) contains the whole length of the 17-amino acid TP sequence and an additional Gly at its COOH terminus. Lengthening TP to an 18-residue, even-numbered peptide TP18 **4** provides a symmetrical antiparallel strand in the cyclic peptide

† This work was supported in part by U.S. Public Health Service NIH Grants CA36544, AI46164, and GM57145.

* To whom all correspondence should be addressed: Department of Microbiology and Immunology, A-5119 MCN, Vanderbilt University, 1161 21st Ave. S., Nashville, TN 37232-2363. Telephone: (615) 343-1465. Fax: (615) 343-1467. E-mail: tamjp@ctrvax.vanderbilt.edu.

10.1021/bi0003487 CCC: $19.00
Published on Web 05/23/2000

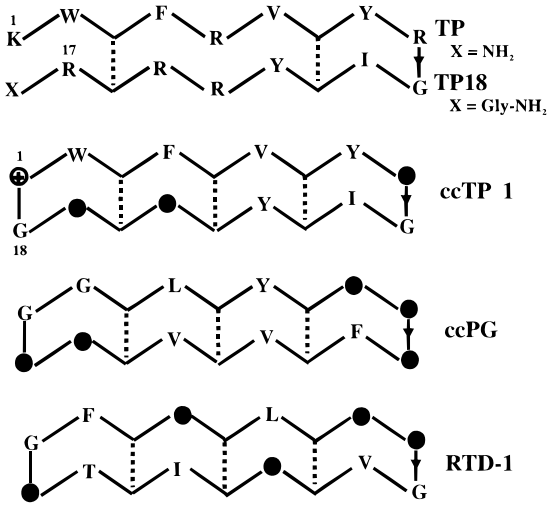

FIGURE 1: Amino acid sequences and topology of a charged amino acid in TP, TP18, ccTP, ccPG, and RTD-1: cationic amino acid (●) Arg and (⊕) Lys and **(- - -)** disulfide bond. The arrow indicates the N to C direction of peptide bonds.

template. TP contains six cationic amino acids and two cross-braced disulfide bonds, whereas ccTP **1** contains only four cationic amino acids. However, ccTP **1** gains two additional constraints through an end-to-end cyclic peptide bond and a third cross-strand disulfide bond by replacing the $Arg^{5,14}$ pair positioned in the middle of the antiparallel β-strands with a $Cys^{5,14}$ pair.

An unusual feature of these naturally occurring and synthetic cyclic tricystine peptides is their pseudosymmetry which is contributed by a closed-chained, two-β-strand structure with three evenly spaced disulfide bonds. From a minimalistic perspective, they approximate a "β-tile"- or "β-tape"-like structure consisting of four consecutively fused cyclic hexapeptides. The up-and-down side chain arrangements on these rigid two-β-strand frameworks produce a top face (arbitrarily assigned) containing clusters of hydrophobic and positive charged amino acids and a sulfur-rich hydrophobic bottom face formed by three cystine pairs.

The combination of rigidity, disulfide motifs, and pseudosymmetry in these β-tile templates affords a structure that maintains amphipathicity through the variable top face and the invariable hydrophobic sulfur-rich bottom face. To correlate the structural requirements of the β-tile ccTP **1** to salt sensitivity, we have examined a panel of peptides **2**−**11** ranging from a rigid cyclic peptide with three covalent constraints to linear peptides with no constraints (Figure 2). To test the importance of rigidity and a cystine core in maintaining the amphipathic design, we have also prepared a second panel of selected [Gly_6] analogues **1a**−**10a** that retain the constraint elements but make drastic sequence changes by replacing all six hydrophobic amino acids with Gly. Gly, the smallest of the 20 genetically coded amino acids, generally disrupts ordered structures in peptides (*30*). Via replacement of six bulky hydrophobic amino acids with six Gly residues, significant changes in physiochemical properties are anticipated, including the disruption of amphipathic structures and the total loss of the hydrophobic amino acid cluster. In this report, we describe the syntheses, conformation, and activity of these two panels of tachyplesin peptides. Our results show that conformational rigidity increases activity under high-salt conditions, while the

1 5 14 18
Lys-*Trp*-Cys-*Phe*-Arg-*Val*-Cys-*Tyr*-Arg-Gly-*Ile*-Cys-*Tyr*-Arg-Arg-Cys-Arg-Gly-NH_2 (TP18)

Number of constraints	Schematic[a] structure	Compound number	Compound name/sequence	[Gly_6]-analogs[b]
IV	1 18	1	ccTP	**1a**
III		2	[$Cys(Acm)^{5,14}$]cTP	**2a**
		3	cTP	**3a**
II		4	TP18	**4a**
		5	[$Cys(Acm)^{7,12}$]cTP	**5a**
		6	[$Cys(Acm)^{3,16}$]cTP	**ND**[c]
I		7	[$Cys(Acm)^{3,16}$]TP18	**ND**[c]
		8	[$Gly^{3,7,12,16}$]cTP	**8a**
0		9	LTP/KWC*FRVC*YR-GIC*YRRC*RG-X	**9a**
		10	rLTP/GYRGIGYRRGR-GKWGFRV-X	**10a**
		11	[Gly_4]rLTP/GYRGIGYR-RGRGKWGFRV-X	**ND**[c]

FIGURE 2: Two analogue series of TP18 4. (a) Sequences TP18 **4** shown on top of the figure. Closed structures represent the end-to-end peptide bond between Lys^1 and Gly^{18}. The arrow indicates the N to C direction of peptide bonds. Cysteine replacements are shown in the compound name. Linear peptide analogues **9**−**11** contain the following sequence: **9**, KWC(Acm)FRVC(Acm)-YRGIC(Acm)YRRC(Acm)RG-X; and **10** and **11**, GYRGIGYR-RGRGKWGFRV-X, where X is thioester $COSCH_2CH_2CONH_2$ in **10** and NHOH in **11**. (b) [Gly_6] analogues contain six Gly replacements at Trp^2, Phe^4, Val^6, Tyr^8, Tyr^{13}, and Ile^{11} shown in italics at the top of the figure. Amino acid sequences of **9a** [KGC-(Acm)GRGC(Acm)GRGGC(Acm)GRRC(Acm)RG-X] and **10a** (GGRGGGGRRGRGKGGGRG-X, where X is $SCH_2CH_2CONH_2$). (c) ND means not done.

combination of conformational rigidity and cystine pairs in the [Gly_6] analogues can maintain amphipathicity and broad-spectrum antimicrobial activity under high-salt conditions. Unexpectedly, these Gly-rich tachyplesin analogues with or without constraints also exhibit specific activity under low-salt conditions against *Escherichia coli.*

MATERIALS AND METHODS

Boc (*tert*-butoxycarbonyl) amino acid derivatives and *N*-hydroxybenzotriazole (HOBt)[1] were obtained from Chemimpex International Inc. (Wood Dale, IL). All solvents, including acetonitrile (CH_3CN), dichloromethane (DCM), dimethylformamide (DMF), dimethyl sulfoxide (DMSO), and 1-methyl-2-pyrrolidinone (NMP), used without additional distillation were obtained from EM Science (Gibbstown, NJ). *N*,*N*′-Dicyclohexylcarbodiimide (DCC), *N*,*N*′-diisopropylethylamine (DIEA), and *p*-cresol were purchased from

[1] Amino acids and the nomenclature of peptide structure are in accordance with the recommendations of the IUPAC-IUB (*J. Biol. Chem. 264*, 668−673). Abbreviations: Acm, acetamidomethyl; CD, circular dichroism; CHCA, α-cyano-4-hydroxycinnamic acid; DCC, *N*,*N*-dicyclohexylcarbodiimide; DCM, dichloromethane; DIC, *N*,*N*-diisopropylcarbodiimide; DIEA, *N*,*N*-diisopropylethylamine; DMF, dimethylformamide; DMSO, dimethyl sulfoxide; HF, hydrofluoric acid; HOBt, *N*-hydroxybenzotriazole; MALDI-MS, matrix-assisted laser desorption ionization mass spectrometry; MBHA resin, methylbenzhydrylamine resin; NMP, 1-methyl-2-pyrrolidinone; RP-HPLC, reverse-phase high-performance liquid chromatography; t_R, retention time; TCEP, tris(carboxyethyl)phosphine; TFA, trifluoroacetic acid; TFE, trifluoroethanol; TSB, trypticase soy broth; SPPS, solid-phase peptide synthesis.

Aldrich Chemical Co. (Milwaukee, WI). α-Chymotrypsin, trypsin, and α-cyano-4-hydroxycinnamic acid were purchased from Sigma Chemical Co. (St. Louis, MO). Trifluoroacetic acid (TFA) was obtained from Halocarbon (River Edge, NJ). Tris(carboxyethyl)phosphine (TCEP) was obtained from Calbiochem (La Jolla, CA). Ultrapure urea was obtained from ICN Biomedical (Costa Mesa, CA). Dialysis membranes was from Spectrum Laboratories, Inc. (Laguna Hills, CA).

Ten organisms obtained from the American Type Culture Collection (ATCC, Rockville, MD) were used for antimicrobial assays. Four Gram-negative bacteria included *E. coli* ATCC 25922, *Pseudomonas aeruginosa* ATCC 27853, *Klebsiella oxytoca* ATCC 49131, and *Proteus vulgaris* ATCC 49132. The three Gram-positive bacteria were *Staphylococcus aureus* 29213, *Micrococcus luteus* ATCC 49732, and *Enterococcus faecalis* ATCC 29212. The three fungi were *Candida albicans* ATCC 37092, *Candida kefyr* ATCC 37095, and *Candida tropicalis* ATCC 37097. The strains were incubated in trypticase soy broth (TSB) which was prepared in double-distilled water and autoclaved for sterilization. TSB was purchased from Becton-Dickinson (Cockeysville, MD).

Peptide Syntheses and Purification. Automated solid-phase peptide synthesis on an ABI 430A peptide synthesizer was performed using Boc chemistry and a single coupling protocol with DCC/HOBt in DMF/NMP (1:1, v/v). Analytical reverse-phase high-performance liquid chromatography (RP-HPLC) was conducted on a Shimadzu LG-6A system with a C_{18} Vydac column (4.6 mm × 250 mm). A linear gradient from 0 to 85% buffer B was run for 30 min at a flow rate of 1 mL/min with detection at 225 nm. Eluent A was 0.04% TFA/H_2O; eluent B was 0.04% TFA/60% CH_3CN/H_2O. Preparative RP-HPLC was performed on a Waters 600 system with a C_{18} Vydac column (22 mm × 250 mm). Matrix-assisted laser desorption ionization mass spectrometry (MALDI-MS) was carried out on a PerSeptive Biosystems Voyager instrument. Samples were dissolved in 1 μL of a 1:2 mixture of H_2O and CH_3CN. Measurements were taken in the linear mode, with α-cyano-4-hydroxycinnamic acid as the matrix.

Preparation of N-Terminal Cysteinyl Peptide Thioester Precursors. All cyclic peptide precursors were assembled by Boc chemistry solid-phase synthesis (*31*, *32*) on Boc amino acid SCH_2CH_2CO-MBHA resin (1 g, 0.26 mmol/g) (*33*, *34*). The cysteinyl protecting groups of these linear precursors were designed with two different protecting group schemes. In method A (peptides **1** and **2** and their corresponding [Gly_4] analogues), chemoselective protection, Cys^5 and Cys^{14} were protected with acetamidomethyl (Acm) and the remaining four with 4-methylbenzyl (MeBzl), and for peptide **3**, one cysteine pair was protected with Acm and the other pair with MeBz. In method B (all other cystine-containing peptides), uniform protection, all cysteines were protected with MeBzl. The assembled peptides were cleaved from the resin (250 mg) by hydrofluoric acid (HF) treatment (9:1 HF/*p*-cresol, v/v, 12 mL) for 75 min at 0 °C. After removal of HF under vacuum and washing with ether to remove the organic scavenger, the crude and deprotected peptides collected on a glass filter funnel were extracted into an 8 M urea solution (pH 7.8, 100 mL) containing TCEP (100 mg). Aliquots of crude unprotected linear peptide thioesters were purified to confirm their identity before cyclization and to determine their rates of cyclization.

End-to-End Cyclization of N-Terminal Cysteinyl Peptide Thioester (35). The 8 M urea solution (150 mL) was dialyzed (MW cutoff of 1000) by sequentially lowering the urea concentration (2000 mL) to 4 M, and then to 2 M to permit concurrent cyclization which was monitored by analytical C_{18} reversed-phase HPLC and MALDI-MS. In general, all cyclization reactions were complete during the 12−18 h dialysis sequence. The dialyzed solution was then diluted with water to 1 M urea (300 mL) for disulfide formation based on the previously described cysteinyl protecting group strategy. In method A, two disulfide bonds (e.g., peptide **1**) were formed by adding 10% DMSO to the peptide urea solution (1 M), and bond formation was complete in 24 h as monitored by HPLC and MALDI-MS. A part of this intermediate was taken for enzymatic digestion to confirm the disulfide bond linkages. To remove the *S*-acetamidomethyl group and to form the third pair of disulfide bonds, the solution was adjusted to pH 4 with acetic acid and 0.1 N HCl, and then nitrogen was bubbled through the mixture for 10 min. An iodine/methanol mixture was then added dropwise until a brown color persisted. The reaction, where the mixture was maintained in a nitrogen atmosphere and in a darkened vessel, was completed in 45 min, as monitored by HPLC and MALDI-MS. The solution was cooled in an ice bath, and excess iodine was quenched by ascorbic acid. The peptide was purified by preparative HPLC in the same manner described above and again characterized by MS. In method B, all disulfide bonds were formed in a 10% DMSO/1 M urea solution for 24−40 h. MALDI-MS measurements were used to determine the identity of these purified cyclic peptides and gave the expected values.

Ag^+-Assisted Cyclization to Synthesis of an End-to-End Cyclic Peptide without a Disulfide Bond. The Ag^+-assisted cyclization method according to Zhang and Tam (*36*) was used to prepare cyclic peptides **8** and **8a**. This method circularized peptides in an end-to-end fashion and used unprotected thioester peptides obtained from the stepwise solid-phase synthesis described previously for the thioester cyclization methods. For the general procedure, linear precursors (peptide thioester) were dissolved in 0.2 M sodium acetate buffer (pH 5.2−5.6) in concentrations ranging from 2 to 20 mM. AgOTfa (3−5 equiv) in DMSO was added to the solution to give a final concentration ranging from 1 to 10 mM. Aliquots were withdrawn for analytical HPLC. Cyclizations were usually complete with 4−20 h. Cyclized peptide was isolated by HPLC and characterized by MALDI-MS. The synthesis of c(KGGGRGGGRGGGGRRGRG) **8a** served as an example of Ag^+-assisted cyclization. The purified peptide thioester, GGRGGGGRRGRGK^{1}GGGRG-$SCH_2CH_2CONH_2$ (1.5 mg, 0.88 μmol, t_R = 16.7 min, MW 1698.7, found 1699.3), was dissolved in a mixed solvent (1.2 mL, pH 5.6, 1:4 sodium acetate buffer/DMSO, v/v). CF_3-COOAg (0.9 mg, 4.09 μmol) was added to the peptide solution. After 36 h, a single peak was obtained via HPLC (t_R = 14.9 min, MW 1593.7, found 1594.1).

Enzymatic Digestion for the Determination of Disulfide Bond Linkages. Disulfide connectivities of cyclic peptide intermediates prepared from method A were determined by α-chymotrypsin or trypsin digestion (*37*), and fragments were determined on target MS analysis (*38*). Trypsin cleavages

on the C-terminal side of lysine and arginine residues and trypsin digestion of **4** yielded two fragments, $WC^{3}(C^{16}R)$-FR ($M + H^{+}$ calcd 886.4, found 886.0) and $VC^{7}(GIC^{12}YR)$-YR ($M + H^{+}$ calcd 1148.5, found 1148.3) that confirmed the $Cys^{3}-Cys^{16}$ and $Cys^{7}-Cys^{12}$ disulfide connectivity. TP contains four aromatic residues, and α-chymotrypsin cleaves the C-terminal side of the aromatic amino acid residues. α-Chymotrypsin digestion of **2** yielded two peptide segments, C(Acm)RC(CF)RGKW (MW calcd 1245.4, found $M + H^{+}$ 1247.1) and C(Acm)VC(YCIGR)Y (MW calcd 1165.8, found $M + H^{+}$ 1167.1), that confirmed the desired parallel cross-strand disulfide motif ($Cys^{3}-Cys^{16}$ and $Cys^{7}-Cys^{12}$) of **2**.

Circular Dichroism (CD) Measurements. CD spectra were recorded on a Jasco J-720 spectropolarimeter over the wavelength range of 250−190 nm using a 1.0 mm path length cell, a bandwidth of 1.0 nm, a response time of 2 s, and averaging over three scans. The spectra are expressed as molar ellipticity [θ].

Antimicrobial Assays. A sensitive and reproducible two-stage radial diffusion assay (*39*) was employed for testing the antimicrobial activity of these peptides. The activities were expressed in units (0.1 mm = 1 unit), and the MICs were determined from the *x*-intercepts of the dose−response curves. Hemolytic activity was determined using fresh human erythrocytes. Peptide concentrations causing 50% hemolysis (EC_{50}) were derived from the dose−response curve (*40*). The membranolytic selectivity index is expressed as EC_{50}/MIC.

RESULTS

Peptide Design. Global and local alterations were used as design elements in the analogue study. In particular, Gly replacements were used in both series of tachyplesin peptides to disrupt conformation and to decrease hydrophobicity. The first series designated **1**−**11** contained TP, ccTP **1**, and 10 other peptides with decreasing constraints. These local alterations based on a graded decrease from four to no constraints permitted the evaluation of conformational rigidity in relation to antimicrobial activity. Two peptides had the three covalent constraints of an end-to-end peptide bond and two cross-strand disulfide bonds; [$Cys(Acm)^{5,14}$]cTP **2** contained a pair of *S*-acetamidomethylated (Acm) Cys derivatives to replace the $Arg^{5}-Arg^{14}$ pair, and the more cationic cTP **3** (c, cyclic) was the cyclic version of TP18 **4**.

TP, TP18 **4**, and two other cyclic peptides (**5** and **6)** contained two constraints. Both TP and TP18 **4** retained the two native disulfide bonds as constraints, while the cyclic [$Cys(Acm)^{7,12}$]cTP **5** and [$Cys(Acm)^{3,16}$]cTP **6** peptides contained only one disulfide bond and a cyclic peptide backbone as constraints. Peptide **7** was an open-chained peptide similar to TP18 **4**, but contained a single disulfide bond as the sole constraint with the outer $Cys^{7}-Cys^{12}$ disulfide bond replaced with two blocked $(Acm)Cys^{3}-Cys^{16}$ derivatives. [Gly_4]cTP **8** with four Cys residues replaced with Gly was constrained by an end-to-end cyclic peptide bond without any disulfide bond and had common design elements that were useful for comparisons with [Gly_6] analogues **1a** and **2a**. As controls, three linear peptides **9**−**11** without any constraints were also prepared. Peptide LTP **9** retained the sequence of TP18 **4** but contained four *S*-alkylated Cys residues as Cys(Acm), while [Gly_4]rLTP **10** contained two global structural alternations: a partially retro sequence (**G**YRGI**G**YRR**G**RGK^{1}W**G**FRV) to cluster cationic charges in a continuous sequence and four Gly residues (in bold) replacing Cys residues. It should be noted that the linear peptides **9** and **10** as well as **9a** and **10a** of the next series were prepared as thioesters. They were linear precursors in our synthetic schemes for preparing various cyclic peptides. The local effect of thioester on **10** was examined in **11**, which contained a polar carboxyl-terminal hydroximate after **10** had been treated with NH_2OH.

A parallel series of eight analogues with global alternations designated **1a**−**10a** contained structural design elements similar to those in the previous series (**1**−**10**), but with six hydrophobic amino acids (Trp^{2}, Phe^{4}, Val^{6}, Tyr^{8}, Tyr^{13}, and Ile^{11}) replaced with Gly to remove the side chain contributions to hydrophobicity. Thus, [Gly_6]ccTP **1a** and [Gly_6]cTP **3a** with Gly replacements for six hydrophobic amino acids corresponded to ccTP **1** and cTP **3** but retained the cyclic and disulfide bonds as constraining elements. Furthermore, the sequences of [Gly_6] analogues were simplified to three types of amino acids and were particularly rich in Gly residues. The most constrained [Gly_6] analogue **1a** contained eight Gly residues (two invariable Gly residues from the TP18 sequence **4**), six Cys residues, and four cationic amino acids, while [Gly_6]cTP **8a** and [Gly_6]-rLTP **10a** contained 12 Gly residues and six cationic amino acids in their sequences and no other types of amino acids.

Syntheses and Characterizations. Open-chained peptides such as TP and TP18 **4** were prepared by the conventional solid-phase methods (*31*, *32*). Cyclic tachyplesin peptides were prepared by orthogonal ligation strategy Cys-thioester and Ag^{+} ion-assisted cyclizations (*34*−*36*). Both cyclization methods employed linear peptide thioesters as precursors obtained by a stepwise solid-phase method, and then the precursors were cyclized to form end-to-end peptide bonds in aqueous solutions to afford the desired products. Cys-thioester cyclization was used to prepare cystine-containing peptides **1**−**3**, **5**, and **6** and their corresponding [Gly_6] analogues, while the Ag^{+} ion-assisted cyclization was used for preparing non-cystine peptides **8** and **8a**. End-group determination was used to confirm the end-to-end cyclic structures (*34*−*36*).

(a) Cys-Thioester Cyclization. The Cys-thioester cyclization was performed in a phosphate buffer at pH 7.6 without the use of any coupling reagent (*34*, *35*). The process was assisted by a thia-zip reaction involving a series of thiol-assisted intramolecular rearrangements. Ultimately, an amino-terminal thiolactone is formed, leading to a spontaneous ring contraction through an *S*,*N*-acyl isomerization which forms the end-to-end peptide bond (*41*). The cyclization rates of these 18-residue macrocyclic peptides were found to be facile, and the reactions were found to be completed in <10 h as monitored by RP-HPLC.

After the cyclization, disulfide bond formation in peptides **1**−**7** and **1a**−**7a** was achieved essentially in a one-pot reaction by adding 10% DMSO to the peptide solution. It was complete in 12 h as monitored by HPLC and MS. For TP, TP18 **4**, and ccTP **1**, chemoselective oxidative disulfide formation for the Cys(Acm) was performed by adjusting the aqueous solution to pH 4 with an acetic acid/0.1 N HCl mixture and treatment with I_2 and methanol to form the desired cystine pair. The crude peptide was purified on

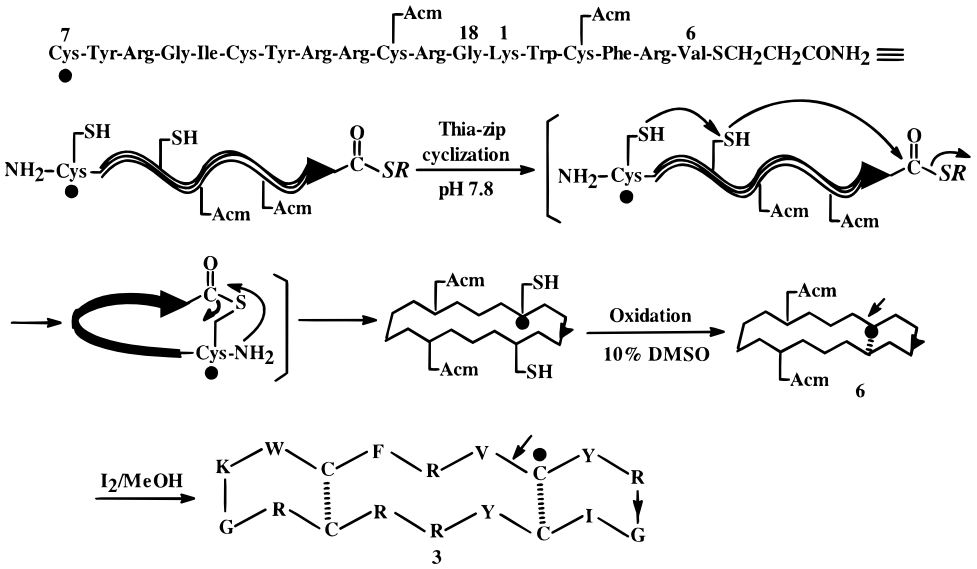

FIGURE 3: Representative synthetic scheme for end-to-end cyclization and disulfide formation of cTP **3**. The thioester peptide was obtained by stepwise synthesis and the cyclic peptide from thia-zip-assisted cyclization. The disulfide bond is first formed by DMSO oxidation. The Cys(Acm) protected disulfide is formed by I_2/CH_3OH. SR is $SCH_2CH_2CONH_2$.

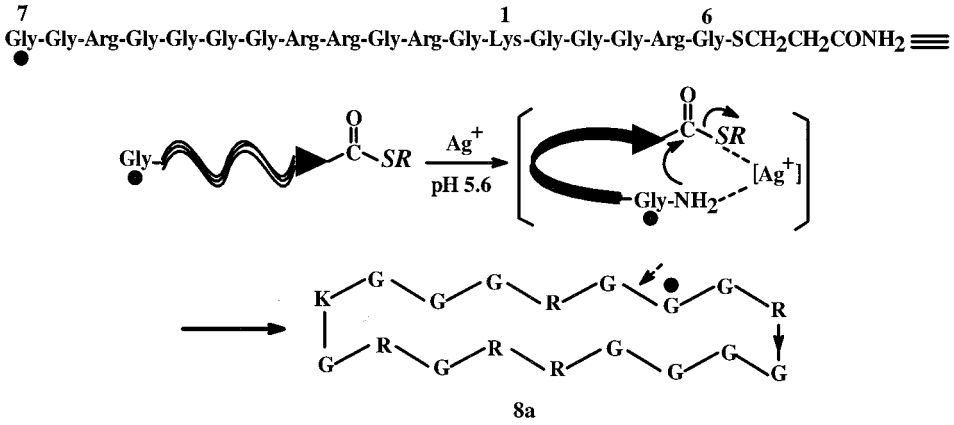

FIGURE 4: Ag^+ ion-assisted orthogonal cyclization to form end-to-end cyclic peptide. The thioester peptide is obtained by stepwise synthesis. SR is $SCH_2CH_2CONH_2$.

preparative HPLC. The disulfide connectivity of peptides **2**−**4** was determined by "on-target" trypsin or α-chymotyrpsin digestion and MALDI mass spectral analysis (*38*).

(b) Ag^+-Assisted Cyclization. This cyclization method was used for preparing cyclic peptides **8** and **8a** without any Cys in their sequences (Figure 4). Cyclization of an unprotected peptide thioester obtained by solid-phase synthesis was performed in an aqueous solution assisted by Ag^+ ion which coordinates the reactive N- and C-terminal thioester ends of an unprotected peptide thioester in forming a cyclic peptide (*36*). Since Gly as an N-terminal amino acid is favored for steric consideration, precursor peptides **8** and **8a** were selected and cyclized (assisted by Ag^+ ion) at pH 5.6 to afford cyclic peptide **8a** in 75% yield.

Hydrophobicity and Amphipathicity As Determined by RP-HPLC. The hydrophobicity of each peptide in both series was determined by its retention time on reverse-phase HPLC. This method of analysis, which is based on the ability of the hydrophobic clusters in a peptide to interact with the hydrophobic surface of the HPLC matrix, has been applied to α-helical and *β*-sheet peptides (*16*, *42*). Thus, the differences due to increases in hydrophobicity can affect retention times. Because the preformed cyclic structure segregates hydrophobic and charge groups in our series, the increase in constraints is also a method for determining amphipathicity. As shown in Table 1, the two series of peptides **1**−**7** and **1a**−**7a**, which essentially share the same sequence, displayed a rough correlation of retention times with increasing constraints, with the highest retention times observed in peptides **1** and **1a**, the most constrained peptides. Peptides **9** and **10** and their corresponding **[**Gly_6] analogues **9a** and **10a** containing carboxyl-terminal thioesters were relatively hydrophobic and displayed retention times similar to those of the more constrained analogous peptides in each series.

Circular Dichroism Measurements. Three types of CD spectra representing different peptides designed in this study were obtained in methanol, water, and phosphate-buffered high-salt solution with 100 mM NaCl at pH 7 (Figure 5). The type I spectra (Figure 5A,A′,D,D′) included the cystine-stabilized peptides of the open-chained TP, TP18 **4**, and monocystine TP **7**. They exhibited two positive bands near 200 and 230 nm and a weak negative band near 208 nm. The positive band ($\pi-\pi^*$ transition) around 200 nm and a weaker negative band ($n-\pi^*$ transition) around 207 nm have been associated with ordered *β*-sheet peptides connected by

Table 1: RP-HPLC Retention Times and Hemolytic Activities

	retention time (min)[a]		hemolytic activity EC_{50} (μM)[b]		selective index (EC_{50}/MIC)[c] 1−11		
peptide	1−11	1a−11a	1−11	1a−11a	Gram-negative bacteria	Gram-negative bacteria	fungi
1, **1a**	24.5	19.1	>450	>450	nc	nc	nc
2, **2a**	21.2	10.6	89	>450	3	34	3
3, **3a**	20.2	13.9	159	>450	398	265	227
TP	20.1	−	91	−	151	130	88
4, **4a**	19.4	11.1	108	>450	360	360	216
5, **5a**	20.1	11.4	151	>500	320	251	189
6	21.4	−	112	−	29	224	140
7	19.4	−	141	−	201	235	235
8, **8a**	18.6	14.9	142	>450	11	11	4
9, **9a**	20.6	12.2	>450	>450	nc	nc	nc
10, **10a**	20.5	14.3	>450	>450	nc	nc	nc
11	20.1	−	>450	−	nc	nc	nc

[a] Gradient from 0 to 85% B over the course of 30 min. [b] Peptide concentrations causing 50% hemolysis (EC_{50}) were derived from the dose−response curves. [c] Mean MIC (micromolar) values under high-salt assays are from Table 2. nc means not calculated; hemolytic activity of >450 μM.

a reverse turn (*43*) and are consistent with the reported CD spectra of TP (*44*, *45*). The strong positive band near 230 nm is usually not observed in β-strand proteins but has been observed in cystine-knot β-strand peptides (*46*). The type II spectra (data not shown) exhibited by the less constrained peptides that included cyclic TP **8**, linear peptides **9**−**11**, and their [Gly_6] analogues contained only a negative band near 200 nm characteristic of predominantly unordered structures in aqueous solution. Similar CD spectra of linear tachyplesin analogues have previously been reported by others (*45*, *47*). The type III spectra exhibited by cyclic and cystine-stabilized ccTP **1**, **1a** (Figure 5A,B), cTP **3**, **3a** (Figure 5C), **4a** (Figure 5D), and **6a** (data not shown) could be considered as nonclassical CD spectra of β-strand structures. These cyclic peptides retained the negative band near 208 nm and the positive band near 230 nm, but exhibited variations in ellipticity below 200 nm. Furthermore, there are substantial differences in their magnitudes as measured by ellipticity and band shifts in their minima and maxima under methanol, water, or phosphate-buffered high-salt conditions. For example, the CD spectra of ccTP **1** and its [Gly_6] analogue **1a** (Figure 5B), which were determined in methanol to avoid peptide aggregation, exhibited a negative band at 203−208 nm, a strong positive band at 228−230 nm, but a weak positive band <200 nm. Under water or high-salt conditions, ccTP **1** exhibited a slightly different spectrum (Figure 5A,B′) with a minimum blue-shifted to 202 nm and the absence of the positive band at <200 nm, whereas the [Gly_6] analogue **1a** exhibited a strong positive band at <200 nm. Tachyplesin is known to behave as a soluble monomeric peptide without any tendency to aggregate in aqueous solutions (*44*), and our results also confirm that there are no significant changes in the CD spectra of TP **1** or TP18 **4** in methanol or water (data not shown). The differences in CD spectra observed under water and high-salt conditions or with methanol suggest the possibility of aggregation of ccTP **1** in low-ionic strength aqueous environments.

At present, there is insufficient information to deconvolute CD spectra of these highly constrained two-β-strand cyclic

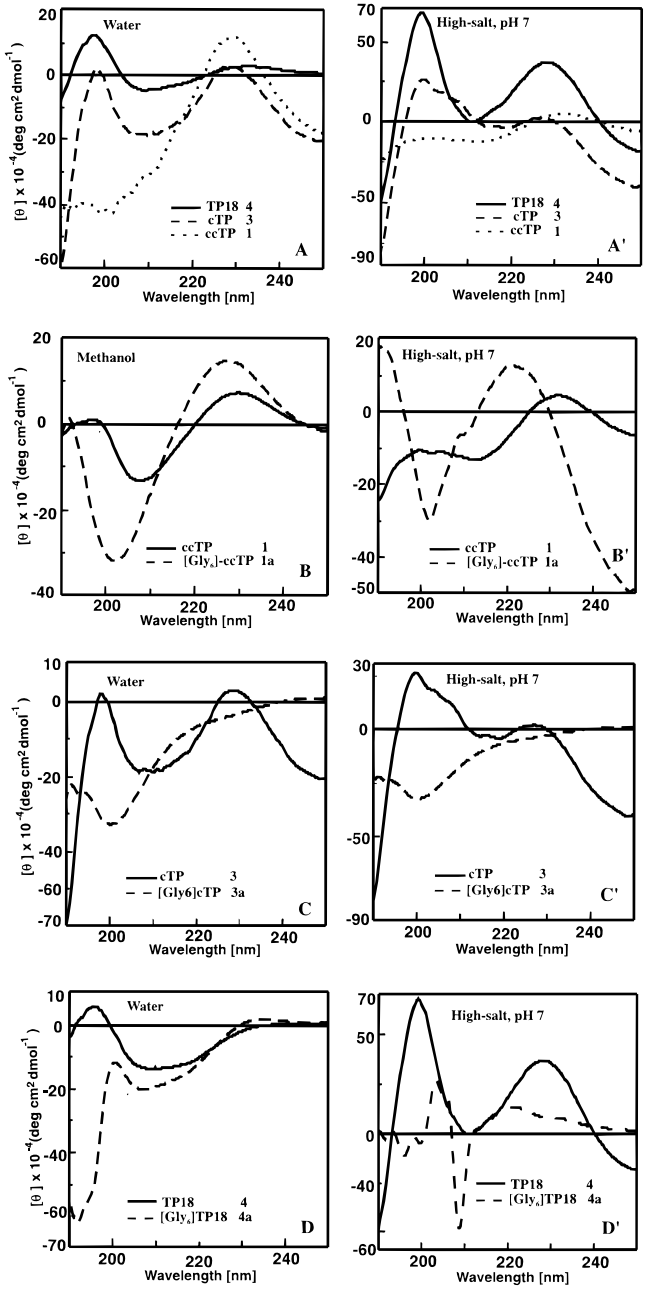

FIGURE 5: CD spectra of tachyplesin and its analogues. High-salt conditions include 100 mM NaCl.

cystine-stabilized structures with unambiguity due to the various contributions by β-turns, aromatic residues, disulfides, and β-sheet structures. Nevertheless, it is reasonable to conclude that the more constrained cyclic peptides **1**−**3** and their corresponding [Gly_6] analogues display some degree of ordered structures in aqueous and high-salt solutions. Furthermore, because the CD profiles of ccTP **1**, [Gly_6]ccTP **1a** in this study, and RTD-1 of Tang et al. (*20*) are very similar, even though their amino acid sequences differ, the rigidity of the cyclic two-strand cystine-knot templates will likely retain a similar ordered structure.

Antimicrobial and Hemolytic Assays. A two-stage radial diffusion assay in agarose gels (*39*) was employed to test the 17-residue TP and its analogues against 10 organisms under both low- and high-salt conditions, with and without 100 mM NaCl, respectively. Each peptide was tested over a 5000-fold range of concentrations, and activities were

Table 2: Antimicrobial Activity of Tachyplesin Peptides 1−11 with Different Constraints[a]

		minimum inhibitory concentration (μM)											
		Gram-negative bacteria					Gram-positive bacteria				fungi			
peptide	salt	*E. coli*	*Pse. aerug.*	*Pr. vulg.*	*K. oxytoca*	mean MIC	*S. aureus*	*M. luteus*	*E. faecalis*	mean MIC	*C. albic.*	*C. kefyr*	*C. tropi.*	mean MIC
1	L	3.0	5.0	6.0	2.1	**4.0**	1.0	0.5	1.0	**0.8**	5.1	3.9	5.2	**4.7**
	H	6.9	5.2	14.4	7.8	**8.6**	0.8	0.4	0.9	**0.7**	17.2	4.1	1.1	**7.5**
2	L	10.7	12.4	5.6	4.0	**8.2**	0.6	1.5	4.6	**2.2**	42.5	10.3	5.2	**19.3**
	H	10.4	34.6	17.8	44.8	**26.9**	5.0	0.9	1.9	**2.6**	72.6	2.8	5.9	**27.1**
3	L	0.1	0.7	0.5	0.4	**0.4**	0.4	1.0	0.3	**0.6**	0.7	0.9	0.5	**0.7**
	H	0.5	0.2	0.8	0.7	**0.6**	0.5	1.1	0.4	**0.7**	0.9	1.3	1.0	
TP	L	0.3	0.9	0.7	0.2	**0.5**	0.4	1.0	0.3	**0.6**	0.7	0.9	0.5	**0.7**
	H	0.4	0.5	1.0	0.5	**0.6**	0.5	1.1	0.4	**0.7**	0.9	1.3	1.0	**1.1**
4	L	0.4	0.5	0.4	0.3	**0.4**	0.4	0.1	0.3	**0.3**	0.2	0.3	0.4	**0.3**
	H	0.1	0.2	0.7	0.2	**0.3**	0.5	0.1	0.4	**0.3**	0.4	0.4	0.8	**0.5**
5	L	0.3	0.6	0.8	0.5	**0.6**	0.9	0.8	0.6	**0.8**	0.2	0.5	0.9	**0.5**
	H	0.4	0.3	0.8	0.4	**0.5**	0.3	0.5	0.9	**0.6**	0.7	0.7	0.9	**0.8**
6	L	0.5	1.1	1.3	0.7	**0.9**	0.8	0.8	NT	**0.8**	1.2	0.7	1.2	**1.0**
	H	9.0	2.8	1.9	1.4	**3.8**	0.5	0.4	NT	**0.5**	0.8	0.7	1.0	**0.8**
7	L	0.5	0.7	0.6	0.4	**0.6**	0.5	0.4	NT	**0.5**	0.4	0.3	0.4	**0.4**
	H	0.1	0.2	1.9	0.4	**0.7**	0.6	0.5	NT	**0.6**	0.7	0.5	0.6	**0.6**
8	L	1.7	1.2	1.1	4.1	**2.0**	4.1	2.3	NT	**3.2**	2.7	1.9	2.3	**2.3**
	H	2.4	20.4	10.5	18.7	**13.0**	4.5	20.2	NT	**12.4**	30.2	40.5	>500[b]	**35.4**
9	L	0.8	0.9	1.1	1.8	**1.2**	0.6	0.6	0.7	**0.6**	1.2	0.5	1.2	**1.0**
	H	0.9	0.6	1.9	1.9	**1.3**	1.0	0.9	1.0	**1.0**	1.9	2.0	1.0	**1.6**
10	L	0.6	1.0	1.4	0.7	**0.9**	1.9	0.9	NT	**1.4**	0.9	1.3	105[b]	**1.1**
	H	1.9	>500[b]	48.0	20.8	**23.6**	1.9	2.0	NT	**2.0**	31.2	73.8	>500	**52.5**
11	L	9.9	12.2	3.0	22.8	**12.0**	50.4	30.4	NT	**40.4**	38.4	15.0	48.0	**33.7**
	H	>500	>500	>500	>500	>**500**	>500	>500	NT	>**500**	>500	>500	>500	>**500**

[a] Experiments were performed via the radial diffusion assay with an underlay gel containing 1% agarose and 10 mM phosphate buffer with (high-salt, H) or without (low-salt, L) 100 mM NaCl. Activities against multiple strains are expressed as the minimum inhibitory concentration (MIC, micromolar). [b] The mean value did not include these data. NT means not tested.

expressed as the minimum inhibitory concentrations (MICs) of 0.1 to >500 μM. As shown in Table 2, TP displayed a broad activity spectrum against 10 test organisms with MICs ranging from 0.2 to 1.3 μM under both low- and high-salt conditions. In the series of peptides **1**−**11**, TP18 **4** was the most active peptide with MICs at 0.1−0.5 μM and exhibited antifungal activity higher than that of TP. Peptides **3**−**10** displayed potencies and activity profiles similar to those of TP under low-salt conditions but produced a larger range of differences under high-salt conditions.

Overall, the cyclic constrained peptides ccTP **1** and [Cys(Acm)^{5,14}]cTP **2** under low- and high-salt conditions were less active than TP against Gram-negative bacteria and fungi. However, ccTP **1** was as active as TP against three test Gram-positive bacteria *S. aureus*, *M. luteus*, and *E. faecalis* with MICs of 1.0, 0.5, and 1.0 μM, respectively, in low-salt and 0.4−0.9 μM in high-salt assays. Peptide **2** exhibited an activity profile similar to that of ccTP **1** with MICs ranging from 0.6 to 4.6 μM against Gram-positive bacteria. The [Gly$_6$] analogues **1a**−**10a** in the parallel series were uniformly less active than TP, and there was a large variation of activity spectra with MICs ranging from 0.7 to >500 μM (Table 3).

We also determined the hemolytic activity on human erythrocytes of both series of peptides (Table 1). The EC_{50} of TP that produced 50% hemolysis of human erythrocytes was 91 μM. Except for peptide **2**, all peptides were less hemolytic than TP, especially those highly constrained and linear peptides with EC_{50}s of >450 μM. Table 1 also compares the membranolytic selectivity indexes (EC_{50}/mean MIC) of peptides **1**−**11**. For simplification, the group-specific mean MICs for Gram-negative bacteria, Gram-positive bacteria, and fungi (see Table 2) were being used to calculate the selective indexes which showed some improvements in cytoxicity over TP under high-salt conditions. The selectivity indexes of [Gly$_6$] analogues **1a**−**10a** were not calculated because the large variations of their MICs would make those indexes statistically unstable.

DISCUSSION

Design, Synthesis, and Conformation. To better understand how to develop salt-insensitive antimicrobial peptides, we have designed tachyplesin peptides with global and/or local changes that include different degrees of constraints and selected corresponding [Gly$_6$] analogues in which all six bulky hydrophobic amino acids were replaced with Gly. Of particular interest are peptide **1** and its globally altered [Gly$_6$] analogue **1a** that contain a β-tile-like framework (Figures 1 and 2) rigidified by three cross-braced disulfide bonds and an end-to-end cyclic peptide bond.

CD measurements in aqueous and high-salt solutions also show that the β-tile peptides **1** and **1a** display ordered structures with characteristics of β-sheet peptides. These two-stranded β-tile-like structures are amphipathic due to positive charges tethered above the plane and a hydrophobic sulfur core of cystine pairs below the plane. Correlation of constraints and amphipathicity based on their elution times on RP-HPLC provides support for this conclusion. Syntheses of cyclic peptides **1**−**8** and **1a**−**8a** are also facilitated by methods using unprotected peptide thioesters that cyclize in aqueous solutions. The thia-zip cyclization method yields cyclic peptides such as **1**−**3** and **1a**−**3a** containing a Cys in their sequences, while the Ag^+-assisted cyclization method provides cyclic peptides such as **8** and **8a** without any Cys

Table 3: Antimicrobial Activity of [Gly_6] Analogues 1a−10a[a]

[Gly_6] peptide	salt	minimum inhibitory concentration (μM)									
		E. coli	*P. aeruginosa*	*Pr. vulgaris*	*K. oxytoca*	*S. aureus*	*M. luteus*	*E. faecalis*	*C. albicans*	*C. kefyr*	*C. tropicals*
1a	L	2.2	1.2	1.9	8.2	7.5	0.7	3.9	4.2	0.9	1.0
	H	1.7	7.8	2.3	18.9	3.0	0.6	19.8	12.4	5.0	5.8
2a	L	2.0	4.7	2.0	54.2	2.4	0.7	20.6	49.8	5.3	5.0
	H	1.7	32.8	2.3	>500	3.0	0.7	54.2	>500	>500	30.2
3a	L	2.1	11.7	13.2	7.8	42.2	30.2	NT	41.0	55.2	>500
	H	>500	>500	>500	>500	>500	>500	NT	>500	>500	>500
4a	L	3.4	1.2	56.5	4.2	7.8	105.2	NT	>500	82.6	18.5
	H	>500	10.9	>500	>500	>500	>500	NT	>500	22.5	>500
5a	L	4.1	11.2	32.8	29.9	42.2	12.4	NT	>500	>500	>500
	H	>500	>500	>500	>500	>500	>500	NT	>500	>500	>500
8a	L	1.9	16.8	8.1	8.9	>500	48.0	NT	>500	>500	>500
	H	>500	>500	>500	>500	>500	>500	NT	>500	>500	>500
9a	L	17.2	22.1	>500	16.0	7.9	>500	NT	>500	>500	>500
	H	>500	>500	>500	>500	>500	>500	NT	>500	>500	>500
10a	L	2.1	4.4	5.3	18.8	30.0	10.5	NT	12.6	17.3	>500
	H	105	>500	>500	>500	>500	48.0	NT	>500	>500	>500

[a] Experiments were performed via the radial diffusion assay with an underlay gel containing 1% agarose and 10 mM phosphate buffer with (high-salt, H) or without (low-salt, L) 100 mM NaCl. Activities against multiple strains are expressed as the minimum inhibitory concentration (MIC, micromolar). NT means not tested.

residues. The advantage of these methods is their simplicity, particularly since cyclic peptides can be obtained without undergoing a deprotection step after the cyclization reaction.

*Cationic Charges and Hydrophobicity in Peptides **1** and **2***. The size and structural constraint elements of the ccTP are similar to synthetic ccPG (Figure 1) and the recently discovered RTD-1 which was isolated from monkey leukocytes (*20*). The cyclic RTD-1 peptide is generated by a novel posttranslational head-to-tail ligation of two truncated α-defensin-like gene products. Our two-β-strand design is also the result of simplification from our previous work on the three-β-strand antimicrobial peptides based on cyclic α-defensins (*48*) and the cyclic cystine-knot circulins (*21*). Topologically, the distributions of hydrophobic and charged clusters of these β-tile templates are different. RTD-1 has an alternating hydrophobic and charged motif, whereas the synthetic ccTP **1** and ccPG contain a central hydrophobic cluster and two charged clusters at the two four-residue reverse turns. Despite their differences in sequences, CD measurements have confirmed that these rigidified cyclic peptides display ordered β-sheet structures (*29*).

In the comparison of the highly constrained antimicrobial peptides, the ratio and topology of cationic and hydrophobic amino acids appear to be important for their activity. ccTP **1** and [$Cys(Acm)^{5,14}$]cTP **2** contains either an extra cystine pair or two *S*-alkylated derivatives that replace a charged Arg pair in their sequences based on TP. As a result, they are less cationic (by two positive charges) and also less active than TP, RTD-1, ccPG, or peptides **3**−**11** in the analogue series. However, ccTP **1** was as potent as TP against the three test Gram-positive bacteria under low- and high-salt conditions. Compared to ccTP **1**, the loss of the cystine constraint in peptide **2** led to a >5-fold loss of potency against *K. oxytoca*, *E. faecalis*, and *C. albicans*.

These results are consistent with the general observation that antimicrobial activity, particularly against Gram-negative bacteria, increases with increasing numbers of cationic charges like those found in the defensin family (*5*, *6*). The decrease in cationic charges coupled with the increase in hydrophobic amino acids also render ccTP **1** and **2** relatively insoluble under assay conditions containing phosphate buffers. In particular, the topology of **1** and **2** containing a continuous stretch of seven hydrophobic amino acids (Trp^2−Tyr^8) occupying one entire β-strand favors aggregation in aqueous solutions and is reminiscent of the highly insoluble β-amyloid peptides (*49*). Thus, our current assay conditions using the overlay gel diffusion method may not accurately portray their antimicrobial activity profile. However, it also likely that increasing the constraints of TP limits its conformational spaces, which results in narrowing its activity spectrum.

*Conformational Constraints and Functional Group Clustering in Peptides **3**−**11***. TP and TP18 **4** exhibit MICs of <0.8 μM against 10 organisms. Unlike tetracationic peptides **1** and **2** and [Gly_4] peptides **8** and **10** in this series, an increase or decrease in conformational constraints in peptides **3**−**7**, **9**, and **10** containing six cationic charges produces a surprisingly small overall effect in their activity spectra under low-salt conditions compared with TP. The more constrained cyclic peptide cTP **3** displays similar potency and activity spectrum under low- and high-salt conditions. Similarly, no large changes in the potency or activity spectrum of the less constrained peptides **5**−**7**, **9**, and **10** can be discerned under low-salt conditions. Under high-salt conditions, there is an increasing loss of potency with decreasing conformational constraints, as observed in peptides **6**, **9**, and **10**. These results suggest that the primary sequence of TP with six bulky amino acids and six cysteines provides the threshold of hydrophobicity for interaction with microbial membranes without any constraint under low-ionic conditions.

*Requirement of Conformational Constraints for High-Salt Activity in Peptides **3**−**11***. TP and TP18 **4** as well as the homologous family of protegrin peptides maintain their conformations via two disulfide bridges that make it possible to compare the importance of constraints for activity under high-salt conditions. The inner disulfide bond (Cys^7−Cys^{12}) has been known to be important in maintaining the β-strand structure. Indeed, the monocystine open-chained TP **7** and the cyclic TP **5** without the outer Cys^3−Cys^{16} disulfide bond did not result in a loss of activity compared to that of TP in low-salt assays. In contrast, removal of the outer disulfide

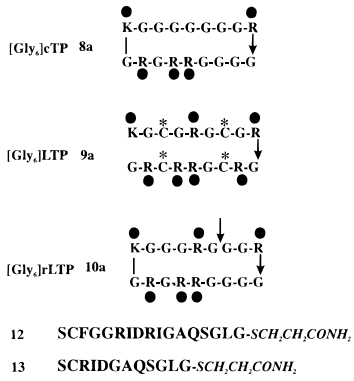

FIGURE 6: Sequences of tachyplesin [Gly_6] analogues **8a**, **9a**, and **10a** and control thioester peptides **12** and **13**. Also shown is the cationic clustering of retro sequences of **10a** in relationship to **9a**: (●) cationic charge and (*) the Cys protected as Cys(Acm) derivatives.

bond in the cyclic TP **6** produced 2−23 lower potencies under high-salt conditions compared to that of TP against all four test Gram-negative organisms, *P. vulgaris*, *K. oxytoca*, *P. aeruginosa*, and *E. coli*.

Peptides **8**−**11** contain both global and local design changes as well as graded hydrophobic differences. The singly constrained peptides **7** and **8** differ in two design elements; peptide **8** contains an end-to-end cyclic structure instead of a cystine pair and four Gly replacements for the Cys derivatives. These combined changes lead to a more flexible [Gly_4] peptide **8** that exhibited a 2−10-fold loss of activity in low-salt assays and a >10-fold decrease in high-salt assays compared to **7**. Peptide **8** essentially lost all its antifungal activity. A similar trend can be discerned in the three linear peptides (**9**−**11**).

Linear peptides **9** and **10** contain a hydrophobic carboxyl-terminal (CT) thioester and global differences in their linear sequences. Peptide **9**, an open chain of TP18 **4**, maintains potent antimicrobial activity against 10 bacteria and fungi under low- and high-salt conditions with MICs at 0.6 and 2.0 μM. The partial retro peptide [Gly_4]rLTP **10** with four Cys → Gly replacements and a 10-amino acid stretch of RRGRGKWGFR, designed to cluster six strong cationic charges in a partial retro sequence, shows a small decrease in potency against eight test organisms under low-salt conditions but is essentially inactive against *C. tropicalis*. Under high-salt conditions, the potency of peptide **10** sharply decreases with most of its MICs in the range of 20 to >500 μM. However, the most significant change in activity was observed between the retro peptides **10** and **11** that contain a small local change at the CT substitution, and peptide **11** bears a hydrophilic hydroximate instead of a thioester. The MICs of peptide **11** decreased >10-fold in seven of nine test organisms under low-salt conditions compared to those of peptide **10**, which was completely inactive under high-salt conditions with an MIC of >500 μM. It is not clear whether the CT thioester plays a functional role in addition to its physiochemical property, but two unrelated basic peptides **12** and **13** containing a CT thioester (Figure 6) did not display any antimicrobial activity against 10 test organisms in our assays (data not shown).

Our results on linear TP peptides are consistent with findings by others. Linear TP with four Cys residues

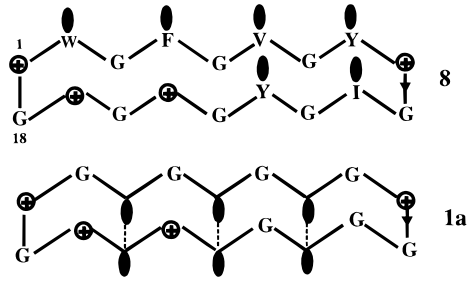

FIGURE 7: Design difference of cyclic peptide with a hydrophobic face on the top (**8**) and on the bottom containing three disulfide bonds (**1a**).

protected by Acm groups (*50*) has been reported to display antimicrobial activity 6.6-fold lower than that of TP against *E. coli*. Furthermore, Rao (*47*) found nearly full activity in several linear TPs with aliphatic amino acids replacing four Cys, which suggests that the two disulfide bonds do not play an important role in their antimicrobial action. However, these assays were performed under low-salt conditions. Thus, our results suggest that the hydrophobic amino acids in tachyplesins play dual structural and functional roles, and while the linear tachyplesin is adequate for membranolytic activity, additional conformational constraints are required for activity under high-salt conditions. Furthermore, our results also show that in the absence of conformational constraints, a small mutation such as the different carboxyl-terminal substitutions in peptides **10** and **11** could lead to a large change in activity.

*[Gly_6] Replacements of Hydrophobic Amino Acids in Analogues **1a**−**10a***. The 17-residue TP contains six bulky hydrophobic acids, four of which are aromatic. Contributions to conformational stability and amphipathicity by single substitutions of these hydrophobic amino acids have been shown to be important to the antimicrobial activity of TP (*47*). Indeed, compared to previous series, the global change of replacing six bulky hydrophobic residues (Trp^2, Phe^4, Val^6, Tyr^8, Ile^{11}, and Tyr^{13}) in the [Gly_6] series (**1a**−**10a**) sharply decreased potency and produced large variations of activity spectra (Table 2). Surprisingly, analogue **1a** was as potent as the parent ccTP **1** under low-salt conditions. In 10 test organisms, the activity of peptide **1a** against seven organisms under low-salt conditions was similar or higher than those ccTP **1**. Under high-salt conditions, peptide **1a** retained similar or exhibited higher activity in six test organisms as compared to that of ccTP **1**. However, other [Gly_6] analogues were far less active than analogue **1a**. With the exceptions of [Gly_6]ccTP **1a** and [Gly_6]($Cys(Acm)^{5,14}$)cTP **2a**, their activities are abrogated in high-salt assays.

In general, there is a rough correlation of activity spectra of the [Gly_6] analogues with the increasing conformational constraints. For the purpose of comparison, we used arbitrary MIC values of 1 and 10 μM as cutoff points for activity criteria against a test organism. Under the 10 μM criterion, the most constrained [Gly_6]ccTP **1a** retains a full active spectrum against 10 test organisms in the low-salt assay and 7 out of 10 organisms in the high-salt assay. Linear analogue **9a** is largely inactive under low-salt conditions except against *S. aureus* (MIC of 7.9 μM) and totally inactive under high-salt conditions (MIC of >500 μM). However, the partial retro sequence of **9a**, [Gly_6]rLTP **10a** with a cationic cluster in

its sequence, is active against three Gram-negative bacteria with MICs of 2.1−5.3 μM. We will discuss analogues **9a** and **10a** later in the section dealing with specificity. The other six [Gly_6] analogues (**3a**−**8a**), with three to one constraints, exhibit activity spectra and potency somewhat similar to those of **10a**. Under the more stringent criterion of 1 μM, [Gly_6]ccTP **1a** is active under low-salt conditions against three organisms, *M. luteus*, *C. kefyr*, and *C. tropicalis*, and active only against *M. luteus* under high-salt conditions. Although [Gly_6]cTP **2a** is active against *M. luteus* under both low- and high-salt conditions (MIC of 0.7 μM), all the other [Gly_6] analogues exhibit activity profiles with an MIC of >1 μM.

Peptides **8** and **1a** share some common global design changes (Figure 7). They contain Gly replacements for either the cystine pairs or six hydrophobic amino acids. [Gly_4]cTP **8** with four Gly residues replacing two cystine pairs retains a cyclic structure. Such a design places both cationic charges and hydrophobic amino acids on the top face but is devoid of the bottom-face sulfur-rich cystine pairs. The [Gly_6] analogue **1a** has the reverse topological amphipathic design which replaces the top-face hydrophobic clusters with Gly but retains the bottom-face sulfur-rich cluster. Thus, it is interesting to find that while peptides **8** and **1a** exhibit comparable activity profiles and potencies under low-salt conditions. However, **1a**, which is more amphipathic (Table 1) and more constrained than **8**, retains its activity under high-salt conditions. Moreover, **1a** ($EC_{50} > 450$ μM) is far less hemolytic than **8** ($EC_{50} = 142$ μM), and it has a higher therapeutic index that is favorable for clinical considerations. Thus, our results suggest that a highly constrained peptide such as **1a** could maintain broad-spectrum activity under both low- and high-salt conditions even without any bulky amino acids in its sequence.

Specificity. Compared to TP, which has an EC_{50} of 91 μM, an increase or decrease of constraints in peptides **3**−**8** results in less hemolytic activity (Table 1). However, the effect is relatively small. In contrast, linear peptides **9**−**11** are nonhemolytic with an EC_{50} of >450 μM and contain the highest selectivity index (EC_{50}/MIC). Since the [Gly_6] analogues **1a**−**10a** are not as active as TP, they are also nonhemolytic with an EC_{50} of >450.

Increased constraints in the [Gly_6] analogues also led to specific recognition of microbial envelopes. The two constrained [Gly_6] analogues **1a** and **2a** are active against *M. luteus* at ≤ 0.7 μM, even under high-salt conditions. Radiolabeled **1a** or **2a** would be useful diagnostically in distinguishing infection from inflammation. Seven [Gly_6] analogues also exhibited moderate but consistent microbial activity against *E. coli* with MICs ranging from 2 to 4 μM under low-salt conditions, irrespective of the number of constraints. The more constrained [Gly_6] analogues **1a** and **2a** can retain their activity under high-salt conditions with an MIC of 1.7 μM. The origin of this specificity is not clear but could be related to the spatial clustering of cationic charges of these cationic Gly-rich sequences (Figure 6). The cyclic constrained nature of **1a**−**4a** and **6a** forms a cluster of cationic charges in the RCRGK sequence. The RRGRGKGGR sequence is found in **8a** and the retro linear peptide **10a** but not in the normal linear peptide, [Gly_6]LTP **9a**, which is considerably less active (MIC of 17.2 μM). It is interesting to note that Gly-rich sequences with weakly cationic clusters are found in microcins (*51*) which are oxazole−thiazole peptide antibiotics with strings of Gly repeats.

Although the generally recognized mechanisms of killing microbes by antimicrobial peptides include their inherent property of membranolytic activity, several antimicrobial peptides have been shown to act on specific targets. Some α-defensins are inhibitors of adrenocorticotrophin receptors and block the production of immunosuppressive adrenal steroid hormones during acute infection (*52*). TP analogues and defensins are also known to be chemoattractants (*53*). Tachyplesin analogues are inhibitors of CXCR4 receptors and are effective as anti-HIV infective agents (*54*). Several β-defensins have now been linked to signal cellular immunity as chemotactic factors in both immature dendritic cells and memory T cells through the CCR6 chemokine receptor (*55*). Insect defensins bind to the Toll family of receptors to mediate antimicrobial response defense (*56*−*58*). The Gly-rich antimicrobial peptide microcin B17 has been shown to be a DNA gyrase inhibitor (*59*), and the bactencin family of peptides with Arg-Pro-rich sequences is believed to have DNA-binding properties (*60*). A recent report by Breukink et al. (*61*) has also shown that the antimicrobial peptide nisin Z is specific for the membrane-anchored cell-wall precursor Lipid II, which is also the target of the conventional antibiotic vancomycin. However, nisin Z binds to Lipid II with high affinity, rendering the plasma membrane more permeable. These specific modes of action by antimicrobial peptides in addition to their nonspecific membranolytic activity provide a new incentive for developing highly rigid antimicrobial peptides selective for targeting specific host or microbial components.

REFERENCES

1. Boman, H. G. (1995) *Annu. Rev. Immunol. 13*, 61−92.
2. Nicolas, P., and Mor, A. (1995) *Annu. Rev. Microbiol. 49*, 277−304.
3. Zasloff, M. (1992) *Curr. Opin. Immunol. 4*, 3−7.
4. Hancock, R. E. (1997) *Lancet 349*, 418−422.
5. Lehrer, R. I., Lichtenstein, A. K., and Ganz, T. (1993) *Annu. Rev. Immunol. 11*, 105−128.
6. Lehrer, R. I., and Ganz, T. (1999) *Curr. Opin. Immunol. 11*, 23−27.
7. Maloy, W. L., and Kari, U. P. (1995) *Biopolymers 37*, 105−122.
8. Wade, D., Boman, A., Wahlin, B., Drain, C. M., Andreu, D., Boman, H. G., and Merrifield, R. B. (1990) *Proc. Natl. Acad. Sci. U.S.A. 87*, 4761−4765.
9. Merrifield, E. L., Mitchell, S. A., Ubach, J., Boman, H. G., Andreu, D., and Merrifield, R. B. (1995) *Int. Pept. Protein Res. 46*, 214−220.
10. Kondejewski, L. H., Farmer, S. W., Wishart, D. S., Kay, C. M., Hancock, R. E. W., and Hodges, R. S. (1996) *J. Biol. Chem. 271*, 25261−25268.
11. Subbalakshmi, C., Krishnakumari, V., Nagaraj, R., and Sitaram, N. (1996) *FEBS Lett. 395*, 48−52.
12. Oh, J. E., Hong, S. Y., and Lee, K.-H. (1999) *J. Pept. Res. 54*, 129−136.
13. Andreu, D., Ubach, J., Boman, A., Wahlin, B., Wade, O., Merrifield, R. B., and Boman, H. G. (1992) *FEBS Lett. 296*, 190−194.
14. Hamuro, Y., Schneider, J. P., and DeGrado, W. F. (1999) *J. Am. Chem. Soc. 121*, 12200−12201.
15. Yakum, T. C., Elzer, P. H., and McLaughlin, M. L. (1996) *J. Med. Chem. 39*, 3603−3605.
16. Kondejewski, L. H., Jelokhani-Niaraki, M., Farmer, W. S., Lix, B., Kay, C. M., Sykes, B. D., Hancock, R. E. W., and Hodges, R. B. (1999) *J. Biol. Chem. 274*, 13181−13192.

17. Dathe, M., Wieprecht, T., Nikolenko, H., Handel, L., Maloy, W. L., MacDonald, K., Beyemann, M., and Bienert, M. (1997) *FEBS Lett. 403*, 208−212.
18. Blondelle, S. E., and Houghten, R. A. (1992) *Biochemistry 31*, 12688−12694.
19. Dathe, M., Shumann, M., Wieprecht, T., Winkler, A., Beyermann, M., Krause, E., Matsuzaki, K., Murase, O., and Bienert, M. (1996) *Biochemistry 35*, 12612−12622.
20. Tang, Y.-Q., Yuan, J., Ösapay, G., Ösapay, K., Tran, D., Miller, C. J., Ouellette, A. J., and Selsted, M. E. (1999) *Science 286*, 498−502.
21. Tam, J. P., Lu, Y.-A., Yang, J.-L., and Chiu, K.-W. (1999) *Proc. Natl. Acad. Sci. U.S.A. 96*, 8913−8918.
22. Gustafson, K. R., Sowder, R. C., II, Henderson, L. E., Parsons, I. C., Kashman, Y., Cardellina, J. H., II, McMahon, J. B., Buckheit, R. W., Jr., Pannell, L. K., and Boyd, M. R. (1994) *J. Am. Chem. Soc. 116*, 9337−9338.
23. Witherup, K. M., Bogusky, M. J., Anderson, P. S., Ramjit, H., Ransom, R. W., Wood, T., and Sardana, M. (1994) *J. Nat. Prod. 57*, 1619−1625.
24. Gran, L. (1970) *Medd. Nor. Farm. Selsk. 12*, 173−180.
25. Gran, L. (1972) *Medd. Nor. Farm. Selsk. 34*, 125−135.
26. Pallaghy, P. K., Niellsen, K. J., Craik, D. J., and Norton, R. S. (1994) *Protein Sci. 3*, 1833−1839.
27. Kokryakov, V. N., Harwig, S. S. L., Panyutich, E. A., Shevchenko, A. A., Aleshina, G. M., Shamova, O. V., Korneva, H. A., and Lehrer, R. (1993) *FEBS Lett. 327*, 231−236.
28. Nakamura, T., Furanaka, H., Miyata, T., Tokunaga, F., Muta, T., Iwanaga, S., Niwa, M., Taokao, T., and Shimonishi, Y. (1988) *J. Biol. Chem. 263*, 16709−16713.
29. Tam, J. P., Lu, Y.-A., and Yang, J.-L. (2000) *Biochim. Biophys. Res. Commun. 267*, 783−790.
30. Richardson, J. S., and Richardson, D. C. (1988) *Science 240*, 1648−1652.
31. Merrifield, R. B. (1963) *J. Am. Chem. Soc. 85*, 2149−2154.
32. Barany, G., and Merrifield, R. B. (1980) in *The Peptides* (Gross, E., and Meienhofer, J., Eds.) Vol. 2, pp 1−284, Academic Press, New York.
33. Hojo, H., and Aimoto, S. (1991) *Bull. Chem. Soc. Jpn. 64*, 111−117.
34. Zhang, L., and Tam, J. P. (1997) *J. Am. Chem. Soc. 119*, 2363−2370.
35. Tam, J. P., and Lu, Y.-A. (1998) *Protein Sci. 7*, 1583−1592.
36. Zhang, L., and Tam, J. P. (1999) *J. Am. Chem. Soc. 121*, 3311−3320.
37. Smyth, D. G. (1967) *Methods Enzymol. 11*, 214−231.
38. Kussmann, M., Nordhoff, E., Rahbek-Nielsen, H., Haebel, S., Rossel-Larsen, M., Jakobsen, L., Gobom, J., Mirgorodskaya, E., Kroll-Kristensen, A., Palm, L., and Roepstorff, P. (1997) *J. Mass Spectrom. 32*, 593−601.
39. Lehrer, R. I., Rosenman, M., Harwing, S. S., Jackson, R., and Eisenhauer, P. (1991) *J. Immunol. Methods 137*, 167−173.
40. Fehlbaum, P., Bulet, P., Machaut, L., Lagueux, M., Broekaert, W. F., Hetru, C., and Hoffmann, J. A. (1994) *J. Biol. Chem. 269*, 33159−33163.
41. Tam, J. P., Lu, Y.-A., and Yu, Q. (1999) *J. Am. Chem. Soc. 121*, 4316−4324.
42. Zhou, N. E., Mant, C. T., and Hodges, R. S. (1990) *Pept. Res. 3*, 8−20.
43. Woody, R. W. (1995) *Methods Enzymol. 246*, 34−71.
44. Oishi, O., Yamashita, S., Nishimoto, E., Lee, S., Sugihara, G., and Ohno, M. (1997) *Biochemistry 36*, 4352−4359.
45. Tamamura, H., Ikoma, R., Niwa, M., Funakoshi, S., Murakami, T., and Fujii, N. (1993) *Chem. Pharm. Bull. 41*, 978−980.
46. Daly, N. L., Love, S., Alewood, P. F., and Craik, D. J. (1999) *Biochemistry 38*, 10606−10614.
47. Rao, A. G. (1999) *Arch. Biochem. Biophys. 361*, 127−134.
48. Yu, Q., Lehrer, R. I., and Tam, J. P. (2000) *J. Biol. Chem. 275*, 3943−3949.
49. Hibich, C., Kisters-Woike, B., Reed, J., Masters, C. L., and Beyreuther, K. (1991) *J. Mol. Biol. 218*, 149−163.
50. Matsuzaki, K., Nakayama, M., Fukui, M., Otaka, A., Funakoshi, S., Fujii, N., Bessho, K., and Miyajima, K. (1993) *Biochemistry 32*, 11704−11710.
51. Bayer, A., Freund, S., Nicholson, G., and Jung, G. (1993) *Angew. Chem., Int. Ed. Engl. 32*, 1336−1339.
52. Solomon, S., Hu, J., Zhu, Q., Belcourt, D., Bennett, H. P., Bateman, A., and Antakly, T. (1991) *J. Steroid Biochem. Mol. Biol. 40*, 391−398.
53. Chertov, O., Michiel, D. F., Xu, L., Wang, J. M., Tani, K., Murphy, W. J., Longo, D. L., Taub, D. D., and Oppenheim, J. J. (1996) *J. Biol. Chem. 271*, 2935−2940.
54. Xu, Y., Tamamura, H., Arakaki, R., Nakashima, H., Zhang, X., Fujii, N., Uchiyama, T., and Hattori, T. (1999) *AIDS Res. Hum. Retroviruses 15*, 419−427.
55. Yang, D., Chertov, O., Bykovskaia, S. N., Chen, Q., Buffo, M. J., Shogan, J., Anderson, M., Schröder, J. M., Wang, J. M., Howard, O. M. Z., and Oppenheim, J. J. (1999) *Science 286*, 525−528.
56. Hoffman, J. A., Kafatos, F. C., Janeway, C. A., Jr., and Ezekowitz, R. A. B. (1999) *Science 284*, 1313−1318.
57. Medzhitov, R., and Janeway, C. A., Jr. (1998) *Proc. Natl. Acad. Sci. U.S.A. 95*, 429−430.
58. William, M. J. (1997) *EMBO J. 16*, 6120−6130.
59. Yorgey, P., Lee, J., Kördel, J., Vivas, E., Warner, P., Jebaratnam, D., and Kolter, R. (1994) *Proc. Natl. Acad. Sci. U.S.A. 91*, 4519−4523.
60. Skerlavaj, B., Romeo, D., and Gennaro, R. (1990) *Infect. Immun. 58*, 3724−3730.
61. Breukink, E., Wiedemann, I., Kraaij, O. P., Kuipers, O. P., Sahl, H.-G., and de Kruijff, B. (1999) *Science 286*, 2361−2364.

BI0003487